IEEE Photonics Journal
An IEEE Photonics Society Publication

Long-Wavelength High-Contrast Grating Vertical-Cavity Surface-Emitting Laser

Volume 2, Number 3, June 2010

Werner Hofmann, Member, IEEE
Chris Chase, Student Member, IEEE
Michael Müller, Student Member, IEEE
Yi Rao, Student Member, IEEE
Christian Grasse
Gerhard Böhm
Markus-Christian Amann, Fellow, IEEE
Connie J. Chang-Hasnain, Fellow, IEEE

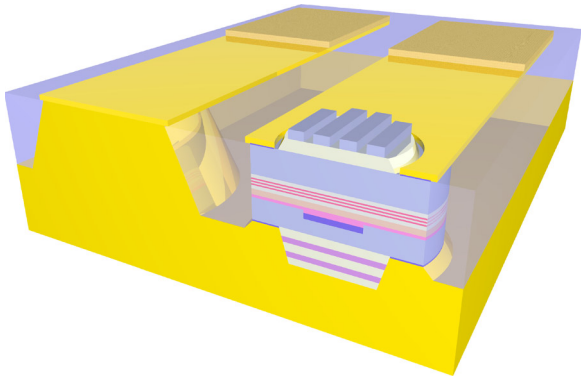

DOI: 10.1109/JPHOT.2010.2049009
1943-0655/$26.00 ©2010 IEEE

IEEE photonics SOCIETY

IEEE

Long-Wavelength High-Contrast Grating Vertical-Cavity Surface-Emitting Laser

Werner Hofmann,[1] *Member, IEEE*, Chris Chase,[1] *Student Member, IEEE*, Michael Müller,[2] *Student Member, IEEE*, Yi Rao,[1] *Student Member, IEEE*, Christian Grasse,[2] Gerhard Böhm,[2] Markus-Christian Amann,[2] *Fellow, IEEE*, and Connie J. Chang-Hasnain,[1] *Fellow, IEEE*

[1]Department of Electrical Engineering and Computer Science, University of California, Berkeley, Berkeley, CA 94720 USA
[2]Walter Schottky Institute, Technical University of Munich, 85748 Garching, Germany

DOI: 10.1109/JPHOT.2010.2049009
1943-0655/$26.00 ©2010 IEEE

Manuscript received February 12, 2010; revised April 14, 2010; accepted April 16, 2010. First published online April 29, 2010. Current version published June 1, 2010. This work was supported by the National Science Foundation through CIAN NSF ERC under Grant EEC-0812072, a National Science Foundation Graduate Research Fellowship supporting C. Chase, and the German Academic Exchange Service (DAAD) for supporting W. Hofmann by a fellowship within the Postdoc Program. Corresponding author: W. Hofmann (e-mail: whofmann@eecs.berkeley.edu).

Abstract: A novel long-wavelength vertical-cavity surface-emitting laser (VCSEL) structure based on a subwavelength high-contrast grating (HCG) as the output mirror has been realized. By design, these devices are highly polarization stable, are single mode at large apertures, and solve the VCSEL-mirror problem at long wavelengths in an elegant way. With cost-effective mass fabrication in mind, the top HCG reflector consists of amorphous silicon on isolator (amorphous silica). The single-mode laser emission is tailored to be around 1320-nm wavelength, targeting applications in high-speed optical data transmission, particularly those for passive optical networks. We report single-mode emission for devices with apertures as large as 11 μm operating in continuous wave with output powers in excess of 0.4 mW. Pulsed operation with output powers up to 4 mW at room temperature is demonstrated as well. This is the first electrically pumped VCSEL structure realized in this wavelength regime utilizing an HCG mirror.

Index Terms: Vertical-cavity surface-emitting laser (VCSEL), high-contrast gratings.

1. Introduction

Vertical-cavity surface-emitting lasers (VCSELs) are preferred light sources in many fields because of their low cost and small packaging capability, single-longitudinal-mode operation with narrow circular beam for direct fiber coupling, 1-D and 2-D arrays defined by lithography, high-speed modulation at low driving currents, and low power consumption. Though the first VCSEL was proposed more than 30 years ago [1], devices in the long-wavelength regime around 1.3 and 1.55 μm with satisfying performance were demonstrated only in the past decade [2]–[8]. The main challenge, compared with VCSELs grown on a GaAs substrate, lies in the difficulty achieving high reflectivity with epitaxial distributed Bragg reflectors (DBRs) lattice-matched on InP, i.e., the substrate of choice for an active region for long-wavelength VCSEL devices. DBRs made with ternary and quaternary alloys have an order of magnitude worse thermal conductivity than the GaAs-Al(Ga)As DBR stacks for the short-wavelength devices. Furthermore, the refractive index contrast is low. This translates, together with the longer wavelengths, into very thick mirrors with large photon penetration depths. This makes devices incorporating *p*-doped epi-mirrors with large electrical and optical losses extremely difficult to

realize. Nevertheless, there has been tremendous progress in the long-wavelength regime using, e.g., hybrid mirrors [5] or wafer-fused GaAs DBR [6] achieving good performance and manufacturability.

However, for many applications, polarization stability has been a challenge for VCSELs, as the structure does not have an intrinsic polarization preference. Prior works to control polarization include using subwavelength surface gratings, transmission gratings or photonic crystal polarizers [9]–[12]. However, the selection is often not strong enough to maintain single polarization during high-speed modulation or when the laser is under certain amount of optical feedback, i.e., an open fiber stub. Subwavelength grating with high refractive index contrast to the surrounding media can provide high broadband reflectivity [13] and various other properties manipulating the lightwave [14].

Recently, we reported a novel subwavelength high-contrast grating (HCG) and its incorporation into a 850-nm VCSEL [15]. We showed that the HCG is ideally suited as a VCSEL mirror, as they provide high and broadband reflectivity for only one polarization. In addition, it has been used to achieve a single fundamental mode with larger apertures than is possible with DBRs. Last but not least, it can replace a 10-μm-thick Bragg-mirror stack by a grating layer in the nanometer range. This kind of reflector seems to be the ideal mirror for VCSELs. Optically pumped device studies [16] and device concepts for short [17] and long-wavelength devices [18] have been published very recently, together with the first tunable HCG VCSEL at shorter wavelengths [19]. However, electrically pumped, long-wavelength HCG VCSELs have not been realized so far.

Here, we present the first long-wavelength HCG VCSEL. The device emits at 1320 nm and is designed for high-speed modulation. The out-coupling mirror is fabricated out of amorphous silicon on isolator material, with the HCG imprinted into the silicon layer and optimized for easy fabrication utilizing state-of-the-art silicon technology. No further DBR layer pairs are used for the mirror. As back-reflector, a hybrid mirror consisting of amorphous dielectrics and metal is deployed. This design is a very elegant solution to the mirror dilemma on long-wavelength VCSELs, additionally solving the key challenges of high-power transverse single-mode emission and polarization stability.

2. HCG Long-Wavelength VCSEL Design

The HCG long-wavelength VCSEL presented here is based on the latest high-speed long-wavelength VCSEL structure with short cavity and record modulation bandwidth [8]. A buried tunnel junction (BTJ), the dimensions of which are precisely controlled by lithography, serves as current aperture. Additionally, due to the BTJ, most of the *p*-conducting material with high electrical and optical losses is replaced by *n*-material. InP, which is a good thermal conductor, is used both at the *n*- and the *p*-side of the device, serving mutually as current and heat spreader. The active region was tailored to emit at 1320 nm: a wavelength for the 10G Ethernet long-range IEEE standard.

At this wavelength, the previous design [5] with an epitaxially grown DBR on InP, showed the biggest challenges. To avoid fundamental absorption in the thick epi-mirror, the aluminum content has to be increased, causing lower refractive index contrast and requiring more mirror pairs. This leads to thicker mirrors with large photon penetration depths causing long photon lifetimes in the cavity with damped RF response. Therefore, we decided to remove all traditional mirrors. The base structure was grown by molecular beam epitaxy (MBE). The aluminum content in the BTJ was raised to avoid fundamental absorption at 1.3 μm. As a consequence, the regrowth was performed by metal-organic chemical vapor deposition (MOCVD) which can tolerate higher aluminum contents. As a reference, a VCSEL structure as published in [7] with a high-index-contrast amorphous DBR mirror consisting of 5 pairs of AlF_3 and ZnS on top was fabricated. Benzocyclobutene (BCB) was used as low-dielectric-constant passivation. However, polarization mode stability is not guaranteed, and higher order transverse modes are not strongly suppressed, as they would be with an HCG.

Therefore, an HCG long-wavelength VCSEL was fabricated on another part of the same epitaxial wafer with a SiO_2 spacer and an HCG of amorphous Si on top. These amorphous layers were deposited by e-beam evaporation; the thickness was controlled by *in situ* white-light reflectometry. The grating was defined by e-beam lithography in a university lab for prototyping; however, could be also done by conventional lithography in a silicon fab for mass fabrication.

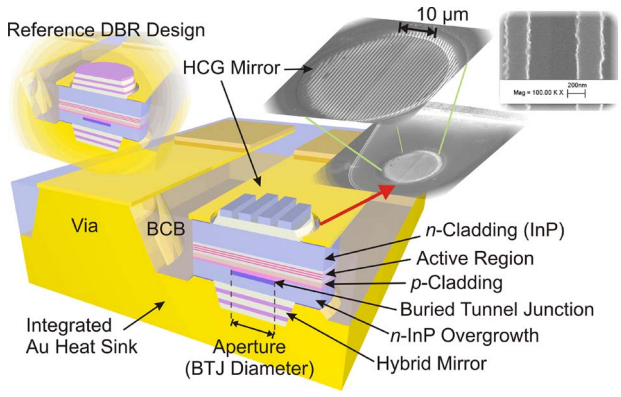

Fig. 1. Cross section of the investigated HCG long-wavelength VCSEL. A microscope image of the processed device and schematic of the reference VCSEL with dielectric DBR as insets. The HCG roughness was with 30 nm quite high and could be improved by process optimization.

The device as described above is presented in Fig. 1 as a schematic, together with the reference design and a scanning electron microscope picture of the fabricated HCG. For the HCG, we fabricated a subwavelength grating with the bars oriented along the [011]-axis of a (100)-InP-wafer, i.e., perpendicular to the large flat. The grating thickness was measured to be 196 nm of silicon; the silica spacer was determined to be 1020 nm. We fabricated gratings with periodicities varying around 820 nm, with bar widths around 200 nm, targeting high reflectivities for transverse electric (TE)-polarized light, i.e., light with electric field components aligned along the grating bars. Due to the amorphous material, some slight roughness below 30 nm had to be tolerated without extensive optimization of the dry-etching process calibrated for crystalline silicon.

3. HCG Reflector Design

Conventional epitaxially grown DBRs are not the mirror of choice for long-wavelength VCSELs. The combination of a hybrid mirror as back-reflector and a HCG mirror as out-coupling mirror is a very elegant way to solve several challenges at one time. HCG reflectors provide very high reflectivity over a wide wavelength range. They can be designed to prefer one polarization and favor the fundamental mode over higher order modes. The HCG design used in this work is different than that used in previous HCG VCSEL work [15], [19]. The HCG is sitting on amorphous silica instead of floating free in air, making it more structurally stable as well as simpler to fabricate. Also, the HCG is made of amorphous silicon, which is slightly lossy $(\alpha = 10\ \text{cm}^{-1})$. Despite the loss, the mirror provides enough reflectivity for the VCSEL to lase. The top mirror in this long-wavelength design also has no additional DBR pairs to aid in providing reflectivity.

Fig. 2 presents the simulated reflection spectra of the HCG used for the VCSEL described in this paper, including loss in the a-Si as measured by photo-thermal deflection. In Fig. 2(a), we can clearly see that the TE-polarized light (solid blue) is highly reflected, whereas TM-polarized light will suffer from large mirror losses. This can very efficiently break the polarization mode degeneracy in VCSELs and provide polarization stability by design. Although, from simulation, the top mirror may have such a high reflectivity that no power is coupled out, we expect practical top reflectivities: This simulation is done assuming plane waves. However, the fundamental mode of a VCSEL is not a plane wave, and just therefore we expect a reasonable amount of power to be coupled out. Further, the HCG has a strong reflectivity dependence as a function of angle (R falls below 99% at just a few degrees off axis) as compared with a DBR (which has a relatively weak dependence on angle). Thus, higher order modes are better suppressed by the HCG than a DBR because they see a lossier top mirror due to their larger transverse *k* vector component. The nature of the high HCG reflectance is quite different from a DBR where in-phase reflectivities add up. In an HCG, the incoming wave excites modes in the grating bars and the air gaps. These modes propagate through the grating and, for certain grating

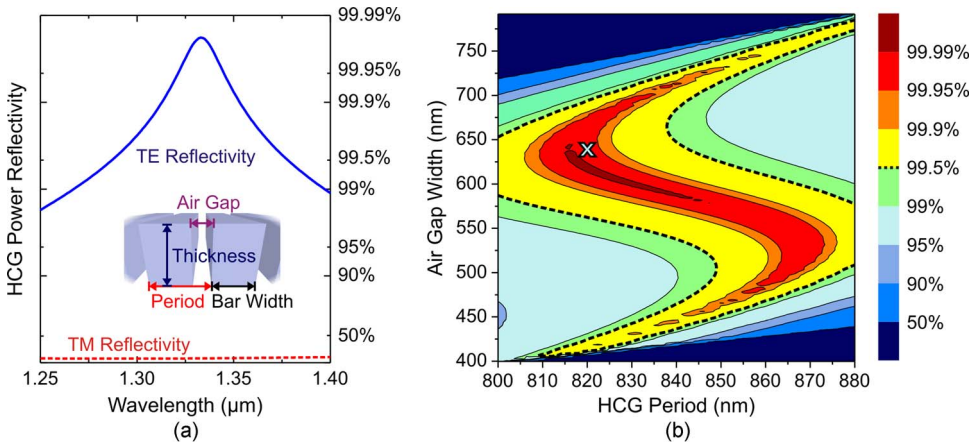

Fig. 2. Simulated HCG reflectivity as deployed on the VCSEL structure presented in Fig. 1. In (a), we plot mirror losses for TE- and TM-polarized light versus wavelength. The reflectivity for TE-polarized light is very high over a wide range, and the TM mode is strongly suppressed. Dimensions are 640-nm air gap and 820-nm HCG period. The thickness was simulated for the measured value of 196 nm. HCG dimensions are labeled in the inset. (b) HCG reflectivity versus design parameters. The grating parameter presented in (a) is marked by an x in (b). The fabrication tolerance for reflectivities larger than 99.5%, which is marked by the dashed line, is expected to be around 100 nm in air gap and 40 nm in period variation.

dimensions, cancel each other out at the other side of the grating. This means they cannot couple into propagating modes at the back side of the grating yielding a very high reflection. The dimensions have to be subwavelength, otherwise light can be diffracted. Depending on the design, HCGs have also a certain phase response, which has to be taken into account for designing the VCSEL cavity. Additionally, a certain minimum spacer is needed to keep near-field components from the grating from coupling power into the underlying laser structure. Fig. 2(b) plots HCG reflectivity for TE-polarized light versus lithographic design parameters at a wavelength of 1325 nm. The HCG was optimized so that it would work even if there was some lithographically induced fabrication error. In this case, a $\pm$20-nm deviation in period and $\pm$50 nm in air gap would still produce a HCG with sufficient reflectivity for the VCSEL to lase. This a-Si HCG design provides a platform, which is easy to integrate into a standard deep ultraviolet lithography mass fabrication process.

4. HCG VCSEL Performance

The HCG long-wavelength VCSELs showed continuous-wave (CW) operation up to 18 °C and pulsed operation up to 60 °C. The CW performance of the HCG VCSEL is presented in Fig. 3. Highly resolved single-mode spectra are depicted in (a) with no visible polarization modes. The setup resolution limit was 0.01 nm and far above the polarization mode splitting of 0.2–0.3 nm. A tuning coefficient is 0.3 nm/mA can be observed. The *LIV* performance is shown in Fig. 3(b) demonstrating CW operation up to room temperature and cooled CW powers in excess of 0.4 mW. Polarization-resolved *LI* measurements were limited by the extinction ratio of our polarizer. The thermal current tuning coefficient is 0.3 nm/mA. Pulsed *L–I*-characteristics are presented in Fig. 4. Devices with an aperture of 17 μm demonstrated powers in excess of 4 mW at room temperature with 200-ns pulse width and a 0.1% duty cycle, as depicted in Fig. 4(a). The 11-μm VCSEL showed low threshold of only 5.6 mA at -15 °C at lases CW up to 18 °C. As shown in Fig. 4(b), the devices operate up to 60 °C and reach their minimum threshold around -30 °C. This proves the first laser operation of an electrically pumped, long-wavelength VCSELs with an HCG as a reflector.

Fig. 5 shows the spectral performance of the devices. The measurement was done by butt-coupling the VCSELs into a multimode fiber and using a conventional optical spectrum analyzer. In Fig. 5(a), we present the spectrum for various device apertures at pulsed current densities of 50 kA/cm^2. Even the 17-μm aperture device shows a side-mode suppression ratio of almost 20 dB. The polarization mode

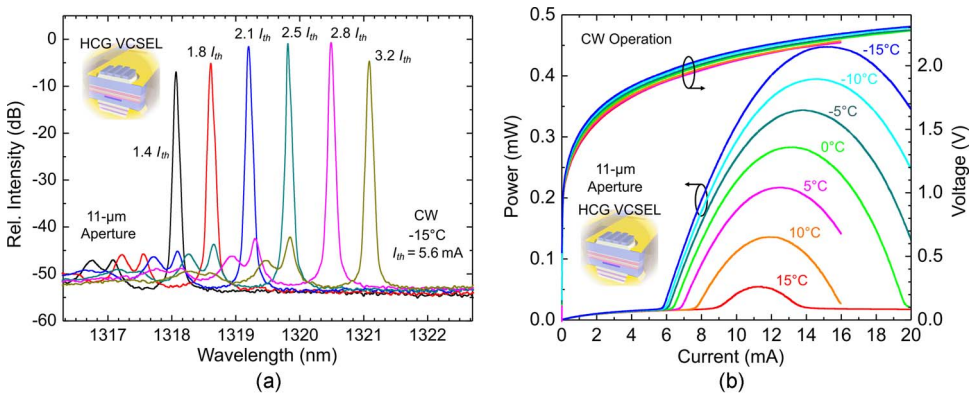

Fig. 3. CW performance of the HCG VCSEL. Highly resolved single-mode spectrum (a) with no visible polarization mode. The tuning coefficient is 0.3 nm/mA. The *LIV* performance (b) shows CW operation above 15 °C and cooled CW powers in excess of 0.4 mW.

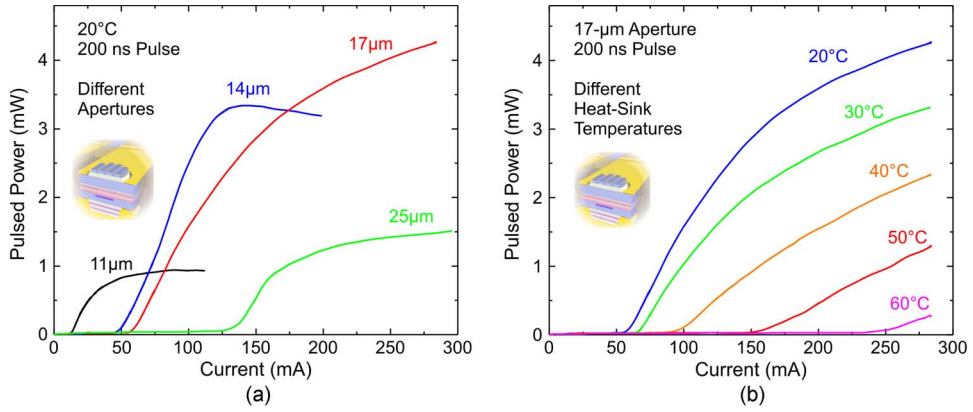

Fig. 4. *L–I* characteristics of the HCG VCSEL for (a) different apertures and (b) different temperatures. The 17-μm aperture device shows a maximum pulsed power in excess of 4 mW for 200-ns pulses. The device with an aperture of 11 μm has a low threshold current and operates CW up to 18 °C. The devices work up to 60 °C and reach the minimum laser threshold value around −30 °C.

is expected to be totally suppressed by design, and could not be observed by our optical spectrum analyzer (0.01-nm setup resolution limit). Fig. 5(b) depicts the spectrum for various heat-sink temperatures. A tuning coefficient of 0.06 nm/K, which has been derived at pulsed operation with constant current densities, can be read out from the inset plotting peak-wavelength versus heat-sink temperature.

5. Discussion

Fabricating the HCG from amorphous material deposited during device manufacturing enabled us to cleave the wafer during the process. So, some of the devices have a dielectric top DBR, while others have the novel HCG reflector. This was done intentionally to be able to experimentally compare the influence of the HCG on VCSEL performance.

The HCG long-wavelength VCSEL presented here were manufactured with a very aggressive design with many changes to the previously published devices of the groups involved, targeting all challenges of these devices. Often, especially for passive optical networks, the VCSEL power is borderline to meet IEEE standards which had edge-emitting laser sources in mind during standardization. This could be solved by pumping larger optical volumes, i.e., larger device apertures. However, above a certain aperture size in VCSELs, higher order transverse modes evolve. Classically, this can be accommodated by lowering the guidance of the optical mode. By using

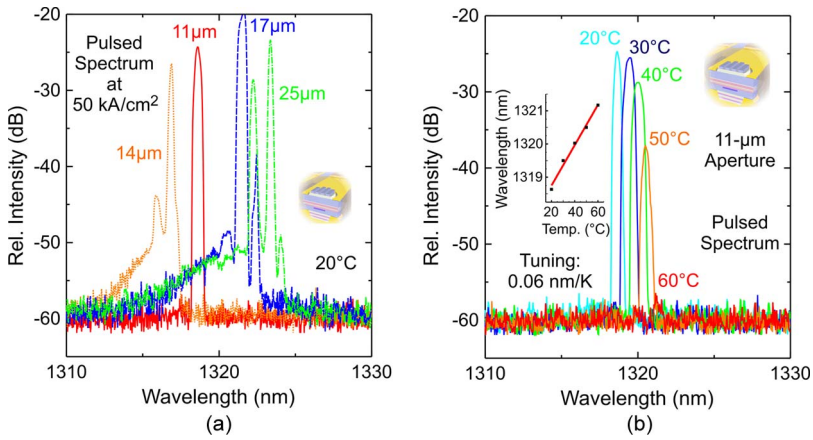

Fig. 5. Pulsed spectra of the HCG long-wavelength VCSEL. In (a), spectra of devices with different aperture diameter ranging from 11 to 25 μm are given. Even the 17-μm aperture device shows a side-mode suppression ratio of almost 20 dB at current densities as high as 50 kA/cm^2. The VCSEL power was coupled to a multimode fiber for measurement. The polarization mode is expected to be totally suppressed by design and could not be observed by our optical spectrum analyzer. In (b), the spectrum is presented for different heat-sink temperatures. Clear single-mode emission can be stated up to 50 °C, and a tuning coefficient of 0.06 nm/K can be read out from the inset.

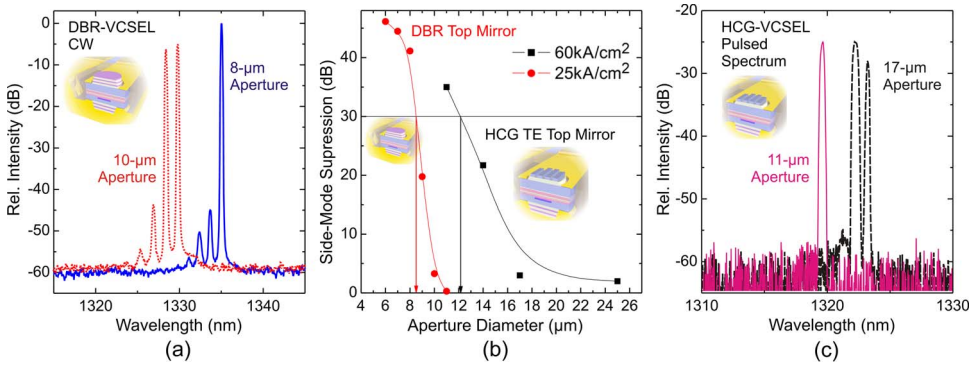

Fig. 6. Influence of the HCG reflector on the single-mode performance of long-wavelength VCSELs: CW spectra of MOCVD regrown DBR VCSELs are presented in (a). Devices with apertures as large as 8 μm are clearly single mode. Replacing the DBR by an HCG reflector pushes devices with apertures up to 12 μm into the single-mode regime (b). This is achieved at current densities that are twice as large. In (c), corresponding pulsed spectra of the HCG VCSELs are presented. All measurements were done at room temperature.

MOCVD regrowth, the index guiding, which is caused by the step of the BTJ defined by dry etching, can almost be eliminated by the planarization properties of MOCVD crystal growth. This caused devices with apertures up to 8 μm to lase single mode with a dielectric mirror, whereas before, with MBE regrowth the largest single-mode devices had apertures around 6 μm. With an HCG reflector, which even further differentiates the fundamental mode, apertures up to 12-μm aperture diameter are in the single-mode regime at wavelengths of 1.3 μm. This is presented in Fig. 6.

In Fig. 6(a), the spectral performance of the reference design is given, and Fig. 6(b) plots side-mode suppression ratio versus aperture diameter for the DBR and the HCG devices. In Fig. 6(c), the pulsed spectra of the HCG devices are presented. Please note that the current densities applied to the HCG devices (pulsed operation for that experiment) were more than twice as high compared with the DBR VCSELs (operating CW below thermal rollover). Therefore, we can expect even larger apertures to be entirely single mode with HCG VCSELs operating CW at lower peak threshold densities.

Changing this many parameters at one time obviously comes at a price. Unlike our MBE chamber, the MOCVD does not have an *in situ* control system for thickness monitoring yet. Layer

thickness and growth rate is calibrated *ex situ* with larger fluctuations compared with the results achieved by our MBE. Since there is a BTJ in the cavity consisting of highly doped, low-bandgap material, the standing cavity wave is very important. Moving the relative location of the BTJ away from a node lets cavity losses raise exponentially. This likely happened to the device presented here, which accounts for higher threshold and poor thermal performance. Further, comparing the emission wavelength of the HCG with the reference VCSELs, one can state a wavelength shift of about 10 nm to the blue side, meaning that the cavity is even further off for the HCG design. This could explain why these novel devices do not perform as well as our previous devices. Further, the reference VCSEL also showed high internal device heating from extensive cavity losses. The small-signal modulation performance at only 14 °C heat-sink temperature resembles the 85 °C results published previously [7] and does not achieve the expected bandwidths well above 15 GHz [8] due to thermal limitations. However, the low-damping, low-photon-lifetime VCSEL cavity still shows excellent high-speed characteristics with bandwidths exceeding 9 GHz. The slope efficiency is only 0.2 W/A for the reference VCSEL and 0.1 W/A for the HCG device accounting for too-high cavity losses rather than too little HCG reflectivity. Of course, also scattering losses from grating imperfections could also be an additional reason to explain the power levels observed. This could be overcome by improving the silicon dry-etch process. On the other hand, because they can still demonstrate CW devices with a detuned cavity, an HCG made from amorphous and slightly lossy material, together with elevated roughness of the HCG sidewalls, further highlights the robustness of the proposed configuration.

Having figured out reasons for temperature-sensitive device performance of this completely novel device, we expect to have a device with much better thermal performance soon by improvements of the MOCVD regrowth, thickness control of the spacer layer, lower HCG roughness, etc. Therefore, we are confident to be able to reproduce operation temperatures up to 120 °C [7] or bandwidths exceeding 15 GHz [8] with this kind of device as well.

6. Conclusion

We presented the first HCG VCSEL structure for the long-wavelength regime. The device is grown on an InP substrate, incorporating a BTJ for a device with low electrical and optical losses and avoiding *p*-material. A hybrid reflector is used as bottom mirror and the light is coupled out via a HCG reflector. The result is an extremely compact VCSEL structure. This mirror design elegantly solves the main challenges for long-wavelength devices with their poor epi-mirrors on InP. Additionally, these lasers are highly single-mode up to aperture diameters as large as 11 μm, suppressing higher order transverse modes. Furthermore, the polarization is determined by design. The grating is manufactured from a silicon layer on silica isolator, targeting cost-effective mass fabrication. The device is manufactured with a low-parasitics, high-speed design and is good for bandwidths well above 10 GHz. For the first attempt pulsed operation at room temperature with peak powers in excess of 4 mW and cooled CW operation with single-mode emission in excess of 0.4 mW could be demonstrated. The HCG design is not limiting the operation temperature. This VCSEL design is a very elegant answer to all major questions for the long-wavelength regime targeting applications for optical data transmission.

References

[1] F. Koyama, "Recent advances of VCSEL photonics," *J. Lightw. Technol.*, vol. 24, no. 12, pp. 4502–4513, Dec. 2006.
[2] M. Ortsiefer, R. Shau, G. Böhm, F. Köhler, and M.-C. Amann, "Low-threshold index-guided 1.5 μm long-wavelength vertical-cavity surface-emitting laser with high efficiency," *Appl. Phys. Lett.*, vol. 76, no. 16, pp. 2179–2181, Apr. 2000.
[3] W. Yuen, G. Li, R. Nabiev, J. Boucart, P. Kner, R. Stone, D. Zhang, M. Beaudoin, T. Zheng, C. He, M. Jensen, D. Worland, and C. Chang-Hasnain, "High-performance 1.6 μm single-epitaxy top-emitting VCSEL," *Electron. Lett.*, vol. 36, no. 13, pp. 1121–1123, Jun. 2000.
[4] N. Nishiyama, C. Caneau, B. Hall, G. Guryanov, M. H. Hu, X. S. Liu, M.-J. Li, R. Bhat, and C. E. Zah, "Long-wavelength vertical-cavity surface-emitting lasers on InP with lattice matched AlGaInAs–InP DBR grown by MOCVD," *IEEE J. Sel. Topics Quantum Electron.*, vol. 11, no. 5, pp. 990–998, Sep./Oct. 2005.

[5] M.-C. Amann and W. Hofmann, "InP-based long-wavelength VCSELs and VCSEL arrays," *IEEE J. Sel. Topics Quantum Electron.*, vol. 15, no. 3, pp. 861–868, May/Jun. 2009.
[6] A. Mereuta, G. Suruceanu, A. Caliman, V. Iacovlev, A. Sirbu, and E. Kapon, "10-Gb/s and 10-km error-free transmission up to 100 °C with 1.3-μm wavelength wafer-fused VCSELs," *Opt. Express*, vol. 17, no. 15, pp. 12 981–12 986, Jul. 2009.
[7] W. Hofmann, M. Müller, A. Nadtochiy, C. Meltzer, A. Mutig, G. Böhm, J. Rosskopf, D. Bimberg, M.-C. Amann, and C. Chang-Hasnain, "22-Gb/s long wavelength VCSELs," *Opt. Express*, vol. 17, no. 20, pp. 17 547–17 554, Sep. 2009.
[8] M. Müller, W. Hofmann, G. Böhm, and M.-C. Amann, "Short-cavity long-wavelength VCSELs with modulation bandwidths in excess of 15 GHz," *IEEE Photon. Technol. Lett.*, vol. 21, no. 21, pp. 1615–1617, Nov. 2009.
[9] S. Schablitsky, L. Zhuang, R. Shi, and S. Chou, "Controlling polarization of vertical-cavity surface-emitting lasers using amorphous silicon subwavelength transmission gratings," *Appl. Phys. Lett.*, vol. 69, no. 1, pp. 7–9, Jul. 1996.
[10] Å. Haglund, J. Gustavsson, J. Bengtsson, P. Jedrasik, and A. Larsson, "Design and evaluation of fundamental-mode and polarization-stabilized VCSELs with a subwavelength surface grating," *IEEE J. Quantum Electron.*, vol. 42, no. 3, pp. 231–240, Mar. 2006.
[11] J. Ostermann, P. Debernardi, and R. Michalzik, "Optimized integrated surface grating design for polarization-stable VCSELs," *IEEE J. Quantum Electron.*, vol. 42, no. 7, pp. 690–698, Jul. 2006.
[12] P. Babu Dayal, N. Kitabayashi, T. Miyamoto, F. Koyama, T. Kawashima, and S. Kawakami, "Polarization control of 1.15 μm vertical-cavity surface-emitting lasers using autocloned photonic crystal polarizer," *Appl. Phys. Lett.*, vol. 91, no. 4, p. 041110, Jul. 2007.
[13] C. Mateus, M. Huang, D. Yunfei, A. Neureuther, and C. Chang-Hasnain, "Ultrabroadband mirror using low-index cladded subwavelength grating," *IEEE Photon. Tech. Lett.*, vol. 16, no. 2, pp. 518–520, Feb. 2004.
[14] Y. Ding and R. Magnusson, "Resonant leaky-mode spectral-band engineering and device applications," *Opt. Express*, vol. 12, no. 23, pp. 5661–5674, Nov. 2004.
[15] M. Huang, Y. Zhou, and C. Chang-Hasnain, "A surface-emitting laser incorporating a high-index-contrast subwavelength grating," *Nature Photon.*, vol. 1, no. 2, pp. 119–122, Feb. 2007.
[16] S. Boutami, B. Benbakir, J.-L. Leclercq, and P. Viktorovitch, "Compact and polarization controlled 1.55 μm vertical-cavity surface-emitting laser using single-layer photonic crystal mirror," *Appl. Phys. Lett.*, vol. 91, no. 7, p. 071105, Aug. 2007.
[17] I.-S. Chung, J. Mørk, P. Gilet, and A. Chelnokov, "Subwavelength grating-mirror VCSEL with a thin oxide gap," *IEEE Photon. Technol. Lett.*, vol. 20, no. 2, pp. 105–107, Jan. 2008.
[18] I.-S. Chung, V. Iakovlev, A. Mereuta, A. Caliman, A. Syrbu, E. Kapon, and J. Mørk, "Selectively-pumped grating-mirror long wavelength VCSEL," in *Proc. IEEE IPRM*, May 2009, pp. 403–405.
[19] C. Chang-Hasnain, Y. Zhou, M. Huang, and C. Chase, "High-contrast grating VCSELs," *IEEE J. Sel. Topics Quantum Electron.*, vol. 15, no. 3, pp. 869–878, May/Jun. 2009.